

STRENGTH AND FATIGUE RESISTANCE OF CLUSTERED SHEAR STUDS



JASON PROVINES



JUSTIN OCEL

BIOGRAPHY

Jason Provines received his BS degree from Michigan State University and MS from Purdue University. He is a Staff Engineer employed by Professional Service Industries, Inc. currently working as a contractor at the Federal Highway Administration Turner-Fairbank Highway Research Center in McLean, VA. His research focus is on fatigue and fracture of steel highway bridges.

Dr. Justin Ocel received his BS degree from the University of Minnesota, MS from Georgia Institute of Technology, and PhD from the University of Minnesota. He is an employee of the Federal Highway Administration working at the Turner-Fairbank Highway Research Facility in McLean, VA as the Structural Steel Research Program Manager. Since arriving at FHWA he has researched a diverse range of topics including creep in epoxy anchors, fatigue strength of ultra-high performance concrete, fatigue of galvanized sign pole details, behavior of steel bridge gusset plated connection, and participating in the NTSB investigation of the I-35W bridge collapse.

SUMMARY

One prefabricated strategy for accelerated bridge construction (ABC) is the use of full depth precast concrete deck panels placed on top of steel girders and connected using shear studs. Pockets, which are cast into the deck panels to fit around the shear studs, are filled with grout to form a composite connection with the steel girder and precast deck panel. For constructability and fabrication purposes, it is advantageous to cluster the studs and increase the distance between these clusters.

To provide composite action between the deck panel and steel beam, the shear stud design must satisfy the strength and fatigue limit states of the AASHTO LRFD Bridge Specifications. Based on a comparison to foreign design provisions and the current test results, the AASHTO shear stud strength provisions appear unconservative, while the fatigue provisions seem too conservative.

This paper describes full-scale static and fatigue tests of composite beams constructed with steel beams and precast concrete decks. The shear stud configurations range from a typical detail with studs spaced every 12 or 24 in. to a detail more conducive to precast panels with cluster spacings of 36 or 48 in., which are currently not permitted by AASHTO. Test results from this research will be used to determine whether clustered shear studs can be placed at extended spacings to facilitate precast decks and to recommend changes, if necessary, to the AASHTO LRFD Bridge Design Specifications.

STRENGTH AND FATIGUE RESISTANCE OF CLUSTERED SHEAR STUDS

Introduction

Prefabricated bridge elements are becoming an increasingly common bridge construction technique in which large modular bridge components are fabricated off-site and then connected together on-site to construct the bridge. One such technique is the use of full-depth precast concrete deck panels placed on top of steel girders and connected via shear studs. The concrete panels typically have pockets to fit around the shear studs, which are then filled with grout to form a composite connection with the girder.

On a typical bridge using conventional cast in place deck, shear studs are regularly spaced along the length of a girder, and have a maximum longitudinal spacing of 24 inches, per the current AASHTO LRFD Bridge Design Specifications (1). When using precast concrete panels, it is advantageous to cluster shear studs closer together and increase the distance between these clusters. Reducing the number of pockets in the deck panels helps simplify panel fabrication and constructability.

To take advantage of composite action between the deck and a steel girder, the shear studs must be designed for the fatigue and strength limit states (1). For short spans (ie. 120' or less) and near the supports, the fatigue limit state can govern the number of studs and requires a significantly larger number of studs than the strength limit state. In some instances, the number of shear studs required

along the length of the bridge leads to a very small longitudinal spacing between studs. An example of this case is shown in Figure 1.

The stud spacing shown in Figure 1 can complicate the use of precast concrete deck panels. As such, this study will include an investigation to see if improvements can be made to better facilitate precast decks. A discussion of the current AASHTO shear stud fatigue and strength design provisions will be presented, as well three international design specifications for shear studs.

Shear Stud Fatigue Design Provisions

The current AASHTO stud fatigue design provisions are based on 44 one-slab push out tests conducted by Slutter and Fisher (1966) using both 3/4 and 7/8 in. diameter shear studs (2). The small-scale test results were compared to beam tests (3 and 4) and it was determined that the lower limit of dispersion (taken as twice the standard error of estimate) of the beam tests was approximately equal to the mean behavior of the push out tests. Therefore, the mean push out fatigue data was used to develop shear stud fatigue design equations (2).

A constant amplitude fatigue limit (CAFL) of 3.5 ksi was later added in 1977 (5) to produce the provisions that are currently being used. No test results were cited as the basis for this addition. The fatigue resistance of a single shear stud is expressed in terms of a shear force range, Z_r (in kips), and is determined using the following equations (1):

For Fatigue I (infinite life):

$$Z_r = 5.5d^2 \quad (1)$$

For Fatigue II (finite life):

$$Z_r = \alpha d^2 \quad (2)$$

in which,

$$\alpha = 34.5 - 4.28 \log N \quad (3)$$

where, d = shear stud diam. (in.), and N = number of cycles.

When compared to other international shear stud fatigue design provisions, the AASHTO provisions



Figure 1. Steel girder with closely spaced studs

appear to be quite different. Figure 2 shows the stud fatigue design curves according to AASHTO (1), the Eurocode 4 (6), Australian Standard (7), and the Japan Society of Civil Engineers (JSCE) (8), all superimposed with the other AASHTO fatigue design curves. Since the JSCE design equation depends on various geometric and material properties, the following typical values were used to compare the provisions: shear stud diameter and height of 7/8" and 6", respectively, and a concrete compressive design strength of 4.0 ksi.

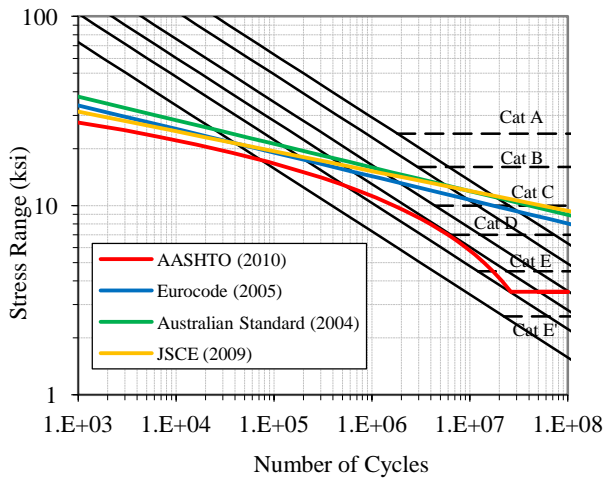


Figure 2. Shear stud S-N design provisions from AASHTO and various international codes

As shown in Figure 2, the AASHTO stud fatigue curve is a semi-log plot, while the other three specifications follow a log-log curve, with slopes varying from -8 to -9.5. These slopes are much shallower than the slope of -3 for the typical AASHTO fatigue details. Since the AASHTO stud curve is semi-log, it becomes much more conservative at a higher number of cycles. This is especially apparent at approximately 26.3 million cycles, where the infinite life fatigue equation governs, and likely where new bridges would be designed. At this large number of cycles, AASHTO requires more than twice as many studs as the other international provisions (9), which suggests AASHTO may be too conservative. The AASHTO stud CAFL of 3.5 ksi also appears to be very conservative, especially since the other international provisions do not have CAFLs for shear studs.

Shear Stud Strength Design Provisions

A shear stud's strength depends on two factors: the resistance of the concrete around the embedded stud

and the resistance of the steel stud itself. The current AASHTO shear stud strength design provisions were developed based on 48 two-slab push out tests conducted by Ollgaard, Slutter, and Fisher (1971) using both 5/8 and 3/4 in. diameter shear studs. Both normal weight and lightweight aggregates were used in the concrete mixes. The small-scale test results were used to develop resistance equations for the concrete around a stud. No recommendations were made regarding the resistance of a stud itself (11).

The resistance of the stud itself was first incorporated into the AASHTO LRFD in its 1st edition in 1994 (12) and into the Standard Specifications in the 2000 Interim Revisions to the 16th Edition (13). No test results were cited as the basis for this addition in either specification. These provisions are the same as those currently being used and are given by the following equation:

$$Q_n = 0.5 A_{sc} \sqrt{f'_c E_c} \leq A_{sc} F_u \quad (4)$$

where, Q_n = shear resistance of shear connector (kips), A_{sc} = cross sectional area of a shear stud (in²), f'_c = concrete compressive design strength (ksi), E_c = modulus of elasticity of concrete, and F_u = specified tensile strength of a shear stud (ksi).

In this equation, the resistance of the concrete surrounding the shear stud is represented by the portion of the equation to the left of the equality, while the portion to the right represents the resistance of a shear stud. Because the shear stud resistance is written in terms of its tensile strength, it implies that a shear stud behaves in pure tension rather than shear, which seems unlikely. When other members, like beams, are designed for shear, a 0.6 (or 0.58) factor is multiplied by the member's tensile strength to determine its shear strength. No such factor is included in Equation (4).

The three international codes all provide similar shear stud strength provisions that include the resistance of the surrounding concrete and the stud itself. However, the Eurocode (6) and Australian (7) provisions both include a 0.8 factor with the stud resistance. This factor implies that shear studs fail somewhere between pure shear and pure tension. Because AASHTO does not include any such factor, a stud's strength could be over-predicted, making the current AASHTO provisions unconservative. This has likely not been an issue because the overly

conservative fatigue provisions make up for the unconservative strength provisions.

The AASHTO provisions also do not provide any guidance for grouping clusters of studs close together to facilitate the use of precast deck panels. All three international codes mention that clustering studs is allowed if consideration is given to account for a greater local demand on the surrounding concrete due to clustering studs, although no explicit guidance is provided (6, 7, and 8). None of the provisions provides guidance to account for shear lag, which would likely be present when using clusters of studs at extended spacings.

Research Objectives

Based on a review of the current domestic and international shear stud specifications, it appears the AASHTO provisions warrant revisiting. The fatigue provisions appear overly conservative, while the strength provisions seem unconservative. In addition, the current AASHTO specifications provide no guidance for placing studs in clusters to facilitate the use of precast concrete deck panels.

This paper will focus on the 17 full-scale tests to be completed using four different configurations of shear pocket spacings welded to 30 ft. long rolled steel beams. The shear stud configurations range from a typical cast in place deck construction detail with studs every 12 or 24 in. to configurations more conducive to precast panels with clustered shear studs spaced at 36 and 48 in. Of the full-scale tests, 5 will be static and 12 will be fatigue tests. A large number of full-scale tests are needed since most of the previous testing was conducted on small-scale tests, including the research used to develop the current specifications.

Experimental Approach

Specimens & Test Setup

The full-scale tests in this study use 30 ft. long W27x84 rolled steel beams. Each beam includes two concrete deck panels fabricated by a PCI certified precaster. The rebar in the deck panels were designed using the empirical deck design in AASHTO (1), and the concrete is a typical DOT deck mix with a compressive design strength of 6.0 ksi. Pockets were cast into the deck panels and were sized depending on the number of studs in each

pocket. Table 1 presents the experimental test matrix with the four different shear stud cluster spacings.

Table 1. Full-scale experimental test matrix

Stud Cluster Spacing	# Long. Shear Studs / Cluster	Total # Studs / Shear Span	# of Static Tests	# of Fatigue Tests
12"	1	24	1	0
12"	1	12	1	3
24"	2	12	1	3
36"	3	12	1	3
48"	4	12	1	3

The number of shear studs in each beam are shown in Table 1 and were designed to induce a shear failure in the studs for the static tests. The beams with 24 and 12 studs per shear span were designed for approximately 75% and 38% composite action, respectively. Since the beams are designed as partially composite, the AISC specifications (14) are used to determine the flexural resistance and rigidity. These calculated values could then be compared to the experimental static test results.

All of the shear studs have a diameter of 7/8 in. and are 6 in. long. These studs were selected due to their use in typical bridge construction. The studs were detailed to penetrate 5 in. into the concrete deck and maintain a cover of 3 in., both of which meet AASHTO Specifications (1). Clustered studs are spaced longitudinally at a pitch of 3.5 in. (4 times the stud diameter, d), which is slightly less than the minimum AASHTO spacing of $6d$. The smaller pitch was chosen to minimize the length of the pockets and is currently allowed in Texas (15). The shear studs were welded onto the steel beams in accordance with AASHTO/AWS D1.5 specifications (16).

Prior to placing the concrete deck panels on the steel beams, the top flange is coated with a thin layer of grease to reduce the amount of friction between the flange and the deck panel so the vast majority of shear force transferred between the steel beam and the deck panels is transmitted through the shear studs. After the deck panels are in place, a series of leveling bolts are used to construct a 1 in. haunch and the haunch formwork is installed. Grout with an expected strength of approximately 8.0 ksi is used to fill the pockets, haunch, and transverse joint in the center of the beam. Grout is mixed and then pumped

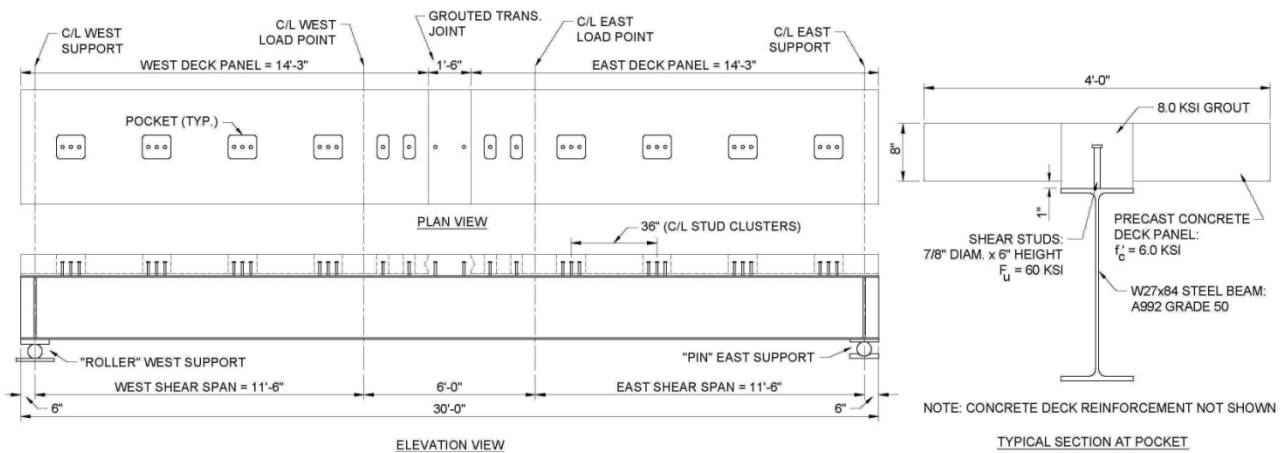


Figure 3. Full-scale test specimen with 36" cluster spacing

into the pockets starting at one end of the beam and finishing at the opposite end.

Figure 3 presents a plan, elevation, and section view of the 36 in. cluster spacing specimen after construction of the beam is completed. Sixteen of the seventeen specimens shown in Table 1 are similar to that shown in Figure 3. The 12 in. spacing specimen with 24 studs per shear span (first line of Table 1) is slightly different from shown in Figure 3. It has two studs, instead of one, placed across the width of the flange to account for twice as many studs as the other specimens. The studs are spaced transversely at 3.5 in. (4d), to meet the AASHTO Specifications (1). The remaining specimens differ only in their number of studs per cluster and cluster spacing.

As shown in Figure 3, each of the fatigue and static specimens have two load points with an 11'-6" shear span on each side of the beam. The fatigue specimens are tested cyclically under load control to produce an initial constant stress range at the base of the studs until the beam reaches failure. The static specimens are tested in displacement control, with the load slowly increasing from zero to a maximum load reached when the specimen fails.

Instrumentation

A large amount of instrumentation is used on each of the specimens, and is basically the same between the static and fatigue tests. The following sections will describe each of these instrumentation types.

Strain Gages

A total of 54 strain gages are used for each full-scale test. Six strain gages are used along four cross

sections on each shear span and one cross section at midspan for a total of nine cross sections. Each section consists of three gages installed on the steel beam and three gages on the concrete deck. Four cross sections along each shear span were chosen to see how well composite action is maintained along the length of the shear span during both static and fatigue testing.

Two sections along each shear span are located at a pocket and two sections are located halfway between pockets. These were chosen to compare how composite action is maintained both at and between pockets. This will help address whether the assumption that plane sections remain plane is valid when using precast deck panels.

Linear Variable Differential Transducers

Twelve linear variable differential transducers (LVDTs) are used on each test. Nine LVDTs are used to measure the relative slip between the concrete deck panel and the top flange of the steel beam. The slip is expected to occur when the shear studs are damaged and eventually fail during the static and fatigue testing. These LVDTs are mounted at the same cross sections where the strain gages are located, and for the same reasons.

Two of the LVDTs measure the relative lift off, or vertical separation, between the deck and the top flange. Lift off is expected to occur when the studs have been damaged such that vertical compatibility no longer exists between the steel beam and the deck. These LVDTs are located in the middle of each shear span. The remaining LVDT is used to measure vertical deflection at midspan of the beam.

FARO Laser Tracker ION

One unique instrumentation feature used on the project is the FARO Laser Tracker ION. This system is somewhat similar to a total station used for surveying; it uses a centralized head unit along with a prism to capture three dimensional coordinates. One major difference is that the FARO automatically tracks the prism rather than the user manually locating it. 3-D coordinates can then be recorded on demand using a remote control. In this instance, the prism is a 0.5 in. diameter steel ball with a spherically mounted reflector that allows coordinates to be measured to an accuracy of 0.0005 in. within an 80 ft. radius of the head. Although the FARO system does not allow for continuous measurement, a large number of discrete measurements can be recorded, where each measurement provides the equivalent of three LVDTs orthogonally mounted at the same location.

For this project, the FARO is used to measure the relative slip and lift off between the grouted haunch and the top flange of the steel beam. This is accomplished by mounting one aluminum spacer to the haunch and one to the edge of the top flange. The FARO instrumentation setup is shown in Figure 4.



Figure 4. Photo of FARO instrumentation on beam

As shown in the figure, the spacers are mounted every 6 in. along the length of the beam for a total of 124 spacers. The prism can then be “nested” into each spacer and its 3-D coordinates can be recorded. Data points are collected at predetermined load and cycle count intervals for the static and fatigue tests, respectively.

Test Results & Discussion

When this paper was written, five of the 17 full-scale tests had been completed. These five include one

static test and four fatigue tests. The results from these tests are discussed in the following sections.

Static Test Results

Testing Procedure

The first static test, referred to as 1S2, was based on a conventional shear stud layout. Studs were placed in transverse pairs with 12 in. longitudinal spacing between pairs for a total of 24 studs per shear span (line 2 of Table 1). This beam was designed for approximately 75% composite action in hopes of producing a horizontal shear failure along the base of the shear studs.

Load was applied using a 220-kip servo-valve hydraulic actuator with a 6 in. stroke at each load point. Load and displacement from each actuator were recorded during testing. A passive lateral bracing system was installed to prevent the beam from moving out of plane. Calcium hydroxide, or “whitewash”, was applied to the middle half of the steel beam to monitor the extent of yielding during testing.

Load was applied at a displacement rate of 0.05 in/min throughout the elastic portion of the test. After some yielding in the beam was observed, the testing rate was increased to 0.1 in/min to speed up the test. The beam was loaded to a displacement of approximately 5.5 in. when the actuators ran out of stroke. Load was then slowly released, steel shim plates were installed between the concrete deck and the actuators, and testing was resumed.

Failure in the beam occurred when loading reached approximately 181.4 kips per load point. The failure occurred due to crushing of the concrete and grout at midspan rather than the desired horizontal shear failure in the shear studs. Nevertheless, some selected data and analysis will be presented.

Visual Observations

Figure 5 shows a photo of beam 1S2 after testing was complete. The crushed concrete and grout at midspan, along with the noticeable deflection in the beam, are shown in the photo. The whitewash showed that at midspan the beam yielded approximately 2/3 up the web and yielding in the bottom flange extended approximately 8 ft. from midspan in both directions. Strain gage data provided good agreement with these visual observations.



Figure 5. Photo of 1S2 completed static test

After testing was complete, the concrete deck panels were removed from the steel beam. A jackhammer was used to remove the grout from the midspan transverse joint and from around the shear studs at the pockets. Visual observations confirmed the three failed studs and significant damage to others. The failed studs were not isolated to one particular location, but were distributed throughout the east shear span. Further examination revealed that the studs behaved in shear with the shear plane located either at the top of the weld flash or at the top of the flange. This is potentially at odds with the current AASHTO Specifications for a stud's strength, which imply shear studs resist forces in pure tension.

Since three studs failed and others exhibited a large amount of shear damage, it is likely that many of the other shear studs were close to failure as well. As shear studs fail, the load per remaining stud increases because the same force must be resisted by a fewer number of studs. It is for this reason the researchers believe the loads encountered during testing were close to those required to cause failure in all of the studs within a shear span.

Strain Gage Results

Strain gage data from the test were used to calculate the maximum horizontal force in both the steel and concrete at failure. The following material properties were used in these calculations and were determined by material testing: $f'_c = 8.0$ ksi (actual concrete strength of deck panel), $f_{y,beam} = 56.6$ ksi, $E_{steel} = 29,000$ ksi, and $f_{u,stud} = 73.5$ ksi. Using strain gage data and these material properties, the maximum horizontal force at each shear span was calculated to be 817 kips. Since there were 24 studs per shear span on beam 1S2, the total horizontal shear stud resistance according to AASHTO is 1060 kips.

Based on the visual observations, it is likely that the 817 kip horizontal force was similar to that required to cause a horizontal shear failure. If this were the case, a factor, which will now be called a shear factor, of approximately 0.8 would need to be applied to the AASHTO shear stud resistance equation to consider that shear studs do not behave in pure tension. Clearly, more than one test result is needed to substantiate using a shear factor of 0.8. However, this shear factor does seem reasonable since two of the international codes reviewed also use a shear factor of 0.8.

Load & Displacement Results

Figure 6 presents a moment-displacement curve for beam 1S2. The midspan moment was calculated using the load from both actuators, and the displacement was taken from the midspan vertical LVDT. As shown in the plot, beam 1S2 reached a maximum midspan moment of 2090 kip-ft. at a displacement of 6.9 in. Also included in Figure 6 are the theoretical elastic stiffness and the moment capacity (M_u) calculated using the AISC Specifications (14).

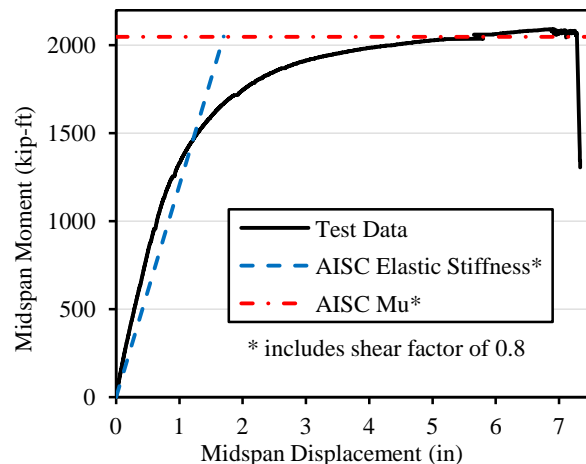


Figure 6. M-Δ data for 1S2 static test

Since the foreign provisions suggested a shear factor of 0.8 should be applied to a stud's strength, this factor was used where necessary when calculating the elastic stiffness and M_u . As shown in Figure 6, the elastic stiffness and M_u calculated using a shear factor of 0.8 provided good agreement with the test data. The slope of the elastic stiffness is relatively similar to the test data up to the additional applied moment to cause yielding, calculated to be 1500 kip-ft. As specified in the AISC commentary (14), 75% of the effective moment of inertia was used when

determining the elastic stiffness to provide realistic deflection calculations.

The moment capacity (M_u), using a 0.8 shear factor, was calculated to be 2050 kip-ft., which is about 2% less than the measured moment reached at failure during testing (2090 kip-ft). If the 0.8 shear factor is not used the moment capacity increases to 2160 kip-ft., which is slightly unconservative when compared to the test results. Because the calculated elastic stiffness and M_u provide good agreement with the test results, applying a 0.8 shear factor to a stud's strength appears reasonable.

Fatigue Test Results

Testing Procedure

To date, four of the twelve planned fatigue tests have been completed. These include one test per each of the four stud cluster spacings. Each of the completed fatigue tests contain 12 studs per shear span and were designed for approximately 38% composite action. This is half the amount as designed for the first static test, 1S2, since only one stud was placed per cross section as shown above in Table 1.

For the fatigue tests, load was applied with the same actuators as used in the static test. The actuators were cycled in load control to produce a desired average stress range at the base of the all of shear studs in each shear span. The loads used during testing allowed for elastic behavior in the beam. The desired stress ranges on the studs were calculated using partial composite action section properties. The beams were cyclically loaded under a constant load range until it was clear that at least one of the precast decks had completely separated from the steel beam.

The naming convention, basic stud geometry, and the stress range on the shear studs of each of the completed fatigue test beams are contained in Table 2. Note the first number in the beam name represents the stud cluster spacing in feet.

Beam Name	Cluster Spacing	# Long. Studs / Cluster	Stud Stress Range (ksi)
1F1	12"	1	20
2F1	24"	2	20
3F1	36"	3	16
4F1	48"	4	20

The 20 and 16 ksi stress ranges were chosen to produce a fatigue failure in the shear studs within a reasonable timeline. One beam will be tested at both of these stress ranges for each cluster spacing. A third stress range, likely less than the first two, will be chosen based on the other fatigue test results. Data and analysis from the four completed fatigue tests will be presented in the following sections.

Visual Observations

After each of the fatigue tests were completed, the concrete deck panels were removed from the steel beam. A jackhammer was used to remove the grout from around the studs at the midspan transverse joint and at other pockets where the studs had not failed. By doing this, the fracture surfaces of the failed shear studs could be examined. Figure 7 presents a photo of the two fracture surfaces of a failed stud.



Figure 7. Photo of shear stud fracture surfaces

As shown in Figure 7 the studs typically failed by a crack initiating at the toe of the weld flash on the midspan side of the stud. The cracks then appeared to propagate down into the top flange leaving a divot as shown in the figure. Dull, smooth surfaces were present on the midspan side of both surfaces indicating fatigue cracking. The cracks appeared more shiny and jagged on the beam end side, indicating fracture. In a few other instances, fatigue cracks initiated at the top of the weld flash on the midspan side of the stud. In these cases, the cracks either propagated through the stud metal or down into the top flange metal until the stud fractured.

Strain Gage Results

Results from the strain gages were used to calculate the location of the neutral axis (N.A.) in both the steel beam and the concrete deck panels throughout fatigue testing. The calculated N.A. locations were then used as a measure of how composite action was affected during cycling. In other words, the location of the N.A. is an indicator of how much damage was being done to the shear studs.

When testing began, the steel beam and concrete decks were expected to behave as one composite section. As the shear studs failed, the steel beam and concrete deck were expected to behave as two separate flexural members on top of one another. Figure 8 presents a plot of the location of the N.A. of different steel cross sections for beam 1F1. The cross sections closest to midspan in each shear span, E4 and W4, are presented in the figure. One section from each shear span was chosen to determine which shear span failed first. The N.A. location for these two sections, along with the midspan section, M, are shown. The composite section and bare steel beam N.A. are also provided for reference.

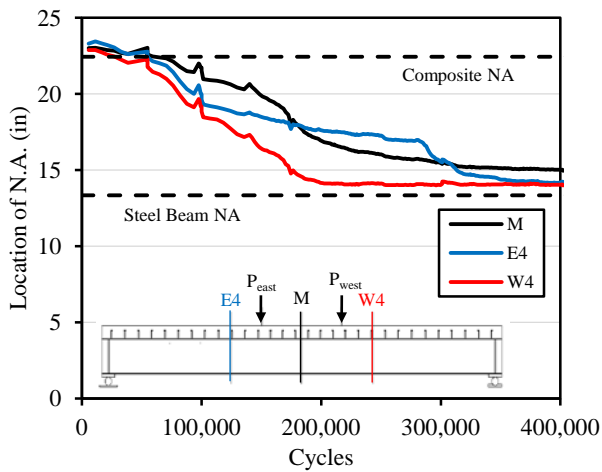


Figure 8. Location of steel neutral axis for east and west shear span sections

As shown in the figure, the N.A. for all three sections start near the composite section N.A. The location of the W4 section N.A. then decreases more rapidly than the other sections until it reaches that of the steel beam at approximately 200k cycles. This shows that composite action in the west section has essentially gone to zero. The location of the E4 section N.A. decreased at a slower rate, but did reach that of the steel beam at approximately 400k cycles.

Since it was determined the west shear span failed first, the cross sections on that side of the beam were examined further. Figure 9 shows the location of the steel beam and concrete deck N.A. for the W4 section. In addition to the composite and bare steel beam N.A., the concrete deck N.A. is included as well.

Similar to the previous plot, Figure 9 shows that both the steel beam and concrete deck begin as a

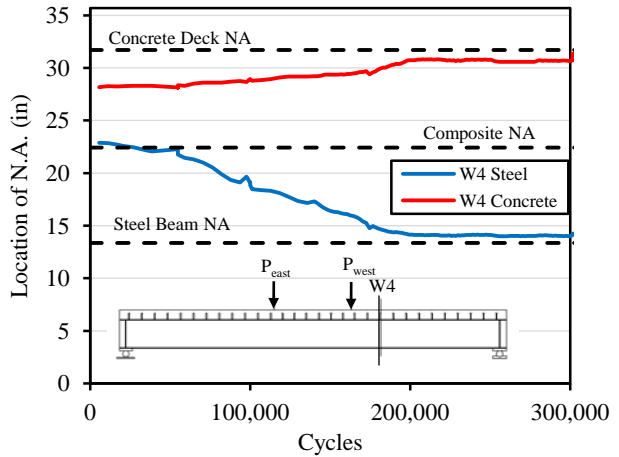


Figure 9. Steel and concrete N.A. locations for section W4 of beam 1F1

composite section. As the number of cycles increases, the location of the N.A. for both elements trend toward their respective noncomposite neutral axes, reaching that point at approximately 200k cycles. Since the location of the N.A. for both elements behave similarly, it suggests that either one can be used as an indicator for the amount of composite action in the beam or as a measure for the fatigue damage being done to the shear studs.

Figure 10 is similar to the other two figures, but includes all four sections on the west shear span since it was shown that the west shear span lost composite action first. The purpose of this figure is to determine if different sections throughout the shear span lost composite action at different times during testing.

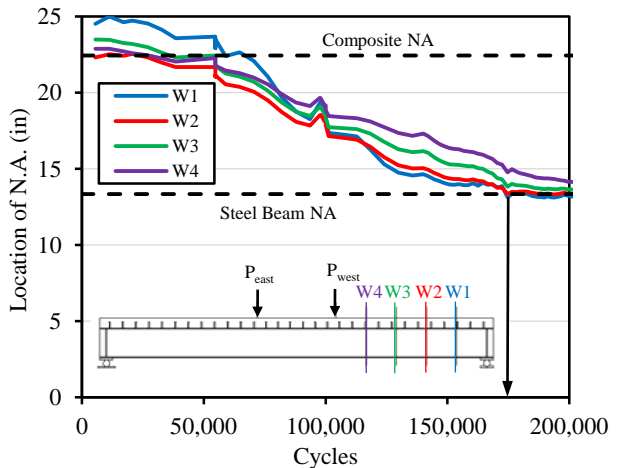


Figure 10. Location of N.A. for west shear span sections of beam 1F1

The four cross sections behave similarly, but the sections closest to the end of the beam (W1, for example) do begin to lose composite action at a slightly faster rate those closer to midspan (W4). This is shown at approximately 100k-150k cycles. During this cycle range, section W1, which is closest to the end, has the lowest N.A. The section second closest to the end, W2, has the second lowest N.A., and so on. This trend seems reasonable since the shear studs closer to the end of the beam have to resist larger a horizontal slip to maintain compatibility than those located closer to midspan.

Although the sections closer to the end of the beam begin to lose composite action at a faster rate, the N.A. of sections W1, W2, and W3 all seem to reach that of the steel beam at the same point, with a cycle count of 175k. This occurs slightly before the section closest to midspan, W4. This section still has some composite action at this point, but its neutral axis does continue to decrease until leveling off at about 200k cycles.

Based on the strain gage data and the location of neutral axes, a definition of failure for the fatigue tests was developed and is as follows: A beam is considered to have reached “failure” if one or more of the cross sections experience a complete loss in composite action. In this case, beam 1F1 failed at 175k cycles. This is shown by the downward vertical arrow in Figure 10.

Beam 2F1 experienced behavior similar to beam 1F1. Composite action was shown to begin to decrease more rapidly in sections closer to the end of the beam than those closer to midspan. All of the sections did, however, seem to reach a point of no composite action at a cycle count of 174k cycles. Beams 3F1 and 4F1 exhibited some differences than the other two beams. For comparison purposes, data from beam 4F1 will be presented.

Figure 11 shows the N.A. locations for the east shear span sections of beam 4F1. Only the east shear span sections are shown because it was determined the east shear span lost composite action before the west shear span. As shown in the beam diagram in the figure, sections E2 and E3 were located halfway between the shear stud clusters, while E1 and E4 were located at the center of the clusters.

Sections E2 and E3 appear to lose composite action faster than the other sections. This is likely because

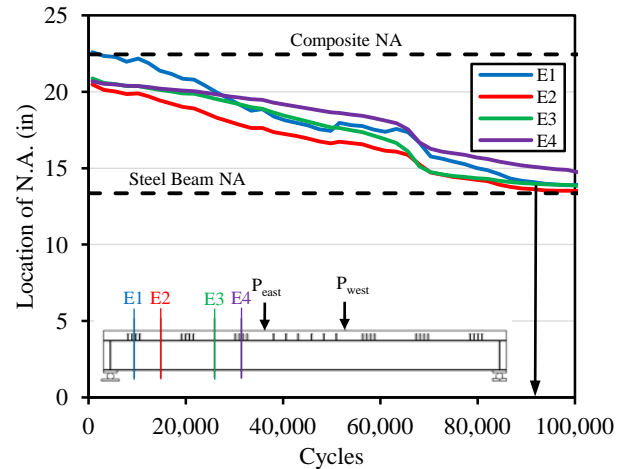


Figure 11. Location of N.A. for east shear span sections of beam 4F1

there are no studs located at these sections. Section E2 does begin to lose composite action slightly faster than section E3 because it is closer to the end of the beam. Similar to beam 1F1, although the sections lose composite action at different rates, the three sections closest to the end of the beam all seem to reach a point of no composite action at the same time. This occurs at 91k cycles and is considered failure for the beam. Similar behavior was also present in beam 3F1. This beam was tested at a smaller stress range of 16 ksi, rather than 20 ksi, and reached a point of failure at 747k cycles.

Using the previously described failure definition, Table 3 was constructed and summarizes the results of the four completed full-scale fatigue tests. The table includes the following information: initial average stress range on all of the shear studs in each shear span, the number of cycles to failure, and which shear span failed first.

Table 3. Completed fatigue test results

Beam Name	Stud Stress Range (ksi)	Cycles	Shear Span Failed
1F1	20	175,000	West
2F1	20	174,000	West
3F1	16	747,000	West
4F1	20	91,000	East

The data contained in Table 3 was used to construct an S-N plot of the test results. This is shown in Figure 12. The AASHTO design equation for shear studs and the typical detail categories are also included in the figure. In the figure, the 12 in. cluster spacing data point is hidden behind the 24 in.

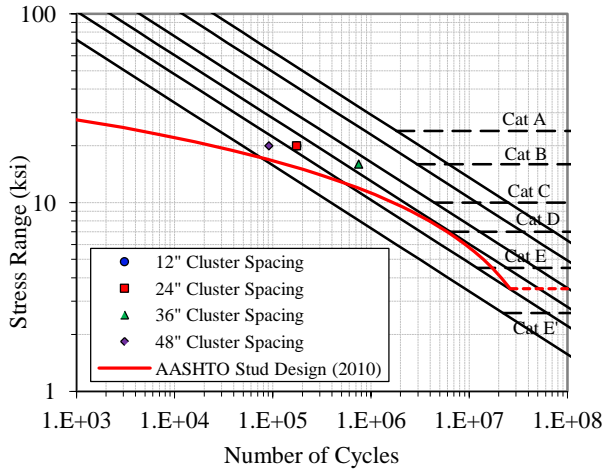


Figure 12. S-N plot of completed full-scale tests

spacing point because the two produced such similar results. All four completed tests fall noticeably above the AASHTO stud design equation. The 48 in. spacing beam did have a fatigue life clearly less than the other two data points at the same stress range. This could be a result of a shear lag effect due to the large cluster spacing, or could simply be due to scatter present in all fatigue data. It is difficult to draw any definitive conclusions because there is only one data point for each of the four cluster spacing beams.

Slip Results

Since the relative slip between the top flange of the steel beam and the grouted haunch was recorded at predetermined cycle intervals, slip damage was observed throughout testing until the beams reached failure. Only FARO data will be presented since this data provided better resolution of slip along the entire length of a beam. The LVDT data did provide reasonably good agreement with the FARO data.

Figure 13 presents the slip data recorded with the FARO laser system for beam 1F1, which has a uniform stud spacing of 12 in. In the figure, slip data were recorded at the maximum load of the fatigue cycles conducted every 100k cycles. Positive values represent a slip toward each respective end of the beam. Values are referenced from measurements taken of the beam under self-weight only. Shaded vertical lines are also included in the figure delineate the locations of the shear stud clusters.

Figure 13 shows that the slip in the beam behaves as expected. Through 100k cycles, the slip remains at approximately zero in the constant moment region at

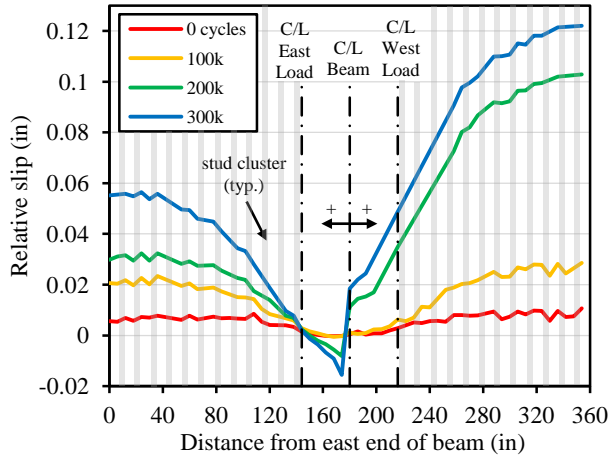


Figure 13. Slip results at peak loads for beam 1F1

midspan and increases gradually on each shear span to reach a maximum value at each end. At 200k cycles, the slip in the west shear span has increased substantially, and it continues to increase through 300k cycles, when it reaches a maximum value of approximately 0.12 in. at the west end of the beam. When the beam reached failure at 175k cycles, the maximum slip was probably slightly less than 0.1 in. It is interesting to note that the slip continues to increase after completely losing composite action. Beam 2F1 displayed similar gradually increasing slip results to those in beam 1F1.

Figure 14 shows the FARO slip results for beam 4F1. Since this was the fourth beam tested, there was a better understanding for the expected fatigue life. Because of this, data were taken every 50k cycles instead of every 100k as was done for beam 1F1. Similar to the previous figure, shaded vertical lines indicate the location of the stud clusters.

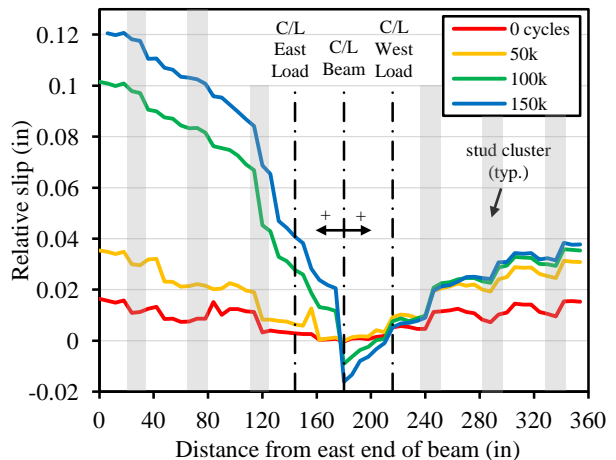


Figure 14. Slip results at peak loads for beam 4F1

The results presented in Figure 14 do appear similar to those shown for beam 1F1. The slip in each shear span is approximately zero near midspan and increases to reach a maximum at each end of the beam. On the east shear span, there is a large amount of slip damage shown at the stud cluster closest to midspan. On the west shear span, however, the slip results almost look like steps. The slip increases at the clusters and remains fairly constant between them. This behavior is expected since the shear studs at the clusters are sustaining damage. When the beam reached failure at 91k cycles, the maximum slip in the east shear span was approximately 0.1 in. The step-like slip behavior was also present in beam 3F1.

Lift Off Results

Similar to the slip results, the FARO laser system data was also used to construct plots of the relative lift off between the top flange and the haunch. The FARO lift off results for beam 1F1 are shown in Figure 15. In the figure, values are referenced from the beam under self-weight only. Positive values indicate the haunch is moving upward from the top flange. Data points were collected at the maximum load of the fatigue cycles every 100k cycles.

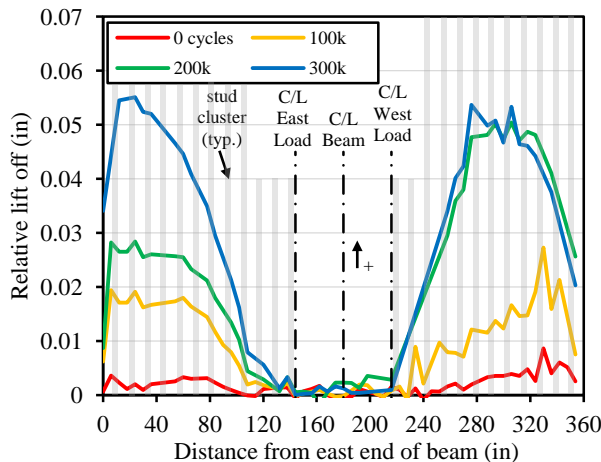


Figure 15. Lift off results at peak loads for beam 1F1

In the plot, no noticeable lift off is present over the constant moment region at midspan. For both shear spans, the lift off then gradually increases toward the end of the beam. It reaches a maximum value at about $\frac{1}{2}$ to $\frac{3}{4}$ of the length of the shear span before decreasing until the end of the beam.

The lift off results support the strain gage data that suggested the west shear span failed first. From the

200k cycle mark, the lift off does not increase any more. This seems reasonable since the beam reached failure at 175k cycles. The east shear span, however, continues to undergo damage since it has not yet reached failure. The lift off reaches a maximum value in the west shear span of approximately 0.05 in. Beam 2F1 exhibited similar behavior as shown by beam 1F1.

For comparison purposes, Figure 16 presents the lift off results for beam 4F1. Data points were collected every 50k cycles. Similar to the previous figure, shaded vertical lines are shown to represent the location of the stud clusters.

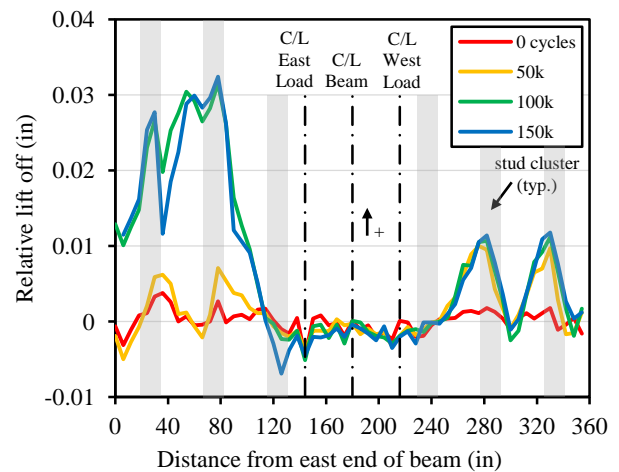


Figure 16. Lift off results at peak loads for 4F1

The most noticeable difference between the lift off results between the two beams is the presence of the peaks. These are most clearly seen in the west shear span, but are also present in the east span as well. The locations of the peaks appear to coincide with the stud clusters. At first, this appears counterintuitive because it seems the lift off should be closer to zero at the clusters and should peak between them.

However, this concept does seem to hold true, just in a different sense. The peaks do tend to occur on the midspan side of each cluster and the lift off decreases to a minimum on the side of the cluster closest to the end of the beam. In other words, the lift off starts at a minimum at the end of a cluster, and it increases to a peak at the beginning of the next cluster. The cluster then acts as an anchor to maintain vertical compatibility between the deck and the steel beam. Similar lift off peaks were also present in beam 3F1.

Summary of Completed Tests

This paper describes the results of limited testing to determine the strength and fatigue resistance of using shear studs in clusters as a means of providing composite action between a steel beam and a precast concrete deck panel. As part of this study, one full-scale static and four full-scale fatigue tests have been completed. The results of the completed static test suggest that a 0.8 factor could be applied to the current shear stud strength provisions.

A failure criterion for shear studs in full-scale fatigue test beams has been defined as a complete loss in composite action, as monitored by the movement of the neutral axis in the steel beam. An S-N plot of results of four different stud cluster spacings is being developed. As expected, shear studs closer to the ends of the beams seem to fail sooner than studs closer to midspan. Composite action also appears to be lost at a faster rate when the shear stud clusters are spaced at greater distances. More test results are needed to develop any further conclusions, but the current AASHTO shear stud provisions appear to be perhaps too conservative for fatigue limit state and unconservative for strength limit state.

Future Work

In addition to completing the remaining full-scale testing as described in the paper, push out tests will also be conducted since these types of tests are the basis for the current AASHTO Specifications. Both static and fatigue push out specimens will be tested so the results can be compared to the full-scale beam tests. Cast in place and precast push out tests will be performed as a means for comparing the two methods of concrete placement.

References

1. AASHTO (2010). AASHTO LRFD Bridge Design Specifications. 5th Edition. American Association of State Highway and Transportation Officials. Washington, D.C.
2. Slutter, R.G., and Fisher, J.W. (1966). "Fatigue Strength of Shear Connectors." *Highway Research Record No. 147*. National Research Council. Washington, D.C.
3. King, D.C., Slutter, R.G., and Driscoll, G.C. (1965). "Fatigue Strength of 1/2 Inch Diameter Stud Shear Connectors." *Highway Research Record No. 103*. National Research Council. Washington, D.C.
4. Toprac, A.A. (1965). "Fatigue Strength of 3/4 Inch Stud Shear Connectors". *Highway Research Record No. 103*. National Research Council. Washington, D.C.
5. AASHTO (1977). Interim Specifications for Bridges. American Association of State Highway and Transportation Officials. Washington, D.C.
6. Eurocode 4 (2005). 1994-2:2005. Design of Composite Steel and Concrete Structures, *Part 2-General Rules and Rules for Bridges*.
7. Australian Standard. (2004). Bridge Design. Part 6: Steel and Composite Construction. Sydney, Australia.
8. Japan Society of Civil Engineers. (2009). Standard Specifications for Steel and Composite Structures. 1st Edition.
9. Lee, K.-C., Abbas, H.H., and Ramey, G.E. (2010). "Review of Current AASHTO Fatigue Design Specifications for Stud Shear Connectors." *Structures Congress 2010 Proceedings*.
10. Fisher, J.W. (1984). "Fatigue and Fracture in Steel Bridges: Case Studies." Wiley. New York.
11. Ollgaard, J.G., Slutter, R.G., Fisher, J.W. (1971). "Shear Strength of Stud Connectors in Lightweight and Normal-Weight Concrete." *AISC Engineering Journal*.
12. AASHTO. (1994). AASHTO LRFD Bridge Design Specifications. 1st Edition. American Association of State Highway and Transportation Officials. Washington, D.C.
13. AASHTO. (2000). Interim Revisions to the 16th Edition Standard Specifications for Highway Bridges. American Association of State Highway and Transportation Officials. Washington, D.C.
14. AISC. (2005). Steel Construction Manual. 13th Edition. American Institute of Steel Construction, Inc.
15. Texas DOT. (2011). Bridge Design Manual – LRFD. Texas Department of Transportation. Revised December 2011.
16. AASHTO/AWS D1.5M/D1.5:2010. (2010). Bridge Welding Code. American Association of State Highway and Transportation Officials & American Welding Society.